

A Eulerian-Lagrangian model to simulate two-phase/particulate flows

By S. V. Apte, K. Mahesh[†], & T. Lundgren[‡]

1. Motivation and Objectives

Figure 1 shows a snapshot of liquid fuel spray coming out of an injector nozzle in a realistic gas-turbine combustor. Here the spray atomization was simulated using a stochastic secondary breakup model (Apte *et al.* 2003a) with point-particle approximation for the droplets. Very close to the injector, it is observed that the spray density is large and the droplets cannot be treated as point-particles. The volume displaced by the liquid in this region is significant and can alter the gas-phase flow and spray evolution. In order to address this issue, one can compute the dense spray regime by an Eulerian-Eulerian technique using advanced interface tracking/level-set methods (Sussman *et al.* 1994; Tryggvason *et al.* 2001; Herrmann 2003). This, however, is computationally intensive and may not be viable in realistic complex configurations. We therefore plan to develop a methodology based on Eulerian-Lagrangian technique which will allow us to capture the essential features of primary atomization using models to capture interactions between the fluid and droplets and which can be directly applied to the standard atomization models used in practice. The numerical scheme for unstructured grids developed by Mahesh *et al.* (2003) for incompressible flows is modified to take into account the droplet volume fraction. The numerical framework is directly applicable to realistic combustor geometries.

Our main objectives in this work are:

- Develop a numerical formulation based on Eulerian-Lagrangian techniques with models for interaction terms between the fluid and particles to capture the Kelvin-Helmholtz type instabilities observed during primary atomization.
- Validate this technique for various two-phase and particulate flows.
- Assess its applicability to capture primary atomization of liquid jets in conjunction with secondary atomization models.

2. Mathematical Formulation

Recent direct numerical simulations of large number of solid particles interacting through a fluid medium by Joseph and collaborators (Choi & Joseph 2001) show that a layer of heavy particles with fluid streaming above it can develop Kelvin-Helmholtz (K-H) instability waves whereas a layer of particles above a lighter fluid develops Rayleigh-Taylor instability. This suggests that the primary breakup of a liquid jet into a spray can be simulated by replacing the jet by a closely packed collection of droplets with some assumed size distribution. The K-H instability at the boundary between droplets and

[†] University of Minnesota

[‡] University of Minnesota, Visiting Fellow Center for Turbulence Research



FIGURE 1. Snapshot spray from a gas-turbine fuel-injector.

fluid would initiate dispersal of droplets into a spray. Further breakup of these dispersed drops can be obtained by advanced secondary breakup models.

The formulation described below is a modification of the equations for spray computation developed by Dukowicz (1980) which consists of Eulerian fluid and Lagrangian particle calculations, and accounts for the displacement of the fluid by the particles as well as the momentum interchange between them. The modifications presented here are mainly in the details of modeling the interaction terms.

2.1. Gas-Phase Equations

The fluid mass for unit volume satisfies a continuity equation,

$$\frac{\partial}{\partial t}(\rho_f \Theta_f) + \nabla \cdot (\rho_f \Theta_f \mathbf{u}_f) = 0 \quad (2.1)$$

where ρ_f , Θ_f , and \mathbf{u}_f are fluid density, volume fraction, and velocity, respectively. This indicates that the average velocity field of the fluid phase does not satisfy the divergence-free condition even if we consider an incompressible suspending fluid. The fluid momentum equation is given as

$$\frac{\partial}{\partial t}(\rho_f \Theta_f \mathbf{u}_f) + \nabla \cdot (\rho_f \Theta_f \mathbf{u}_f \mathbf{u}_f) = -\nabla(\Theta_f p) + \nabla \cdot (\mu_f \mathbf{D}_c) + \mathbf{F} \quad (2.2)$$

where p is the average dynamic pressure in the fluid phase, μ_f is the viscosity of the fluid phase, and $\mathbf{D}_c = \nabla \mathbf{u}_c + \nabla \mathbf{u}_c^T$ is the average deformation-rate of the fluid-particle composite, \mathbf{u}_c is the composite velocity of the mixture, and F is the force per unit volume the particles exert on gas. These equations are derived in detail for constant density flows by Joseph & Lundgren (1990). For particulate flows and dilute suspensions at low Reynolds numbers, the fluid viscosity should be replaced by an effective viscosity μ^* by using Thomas (1965) correlation,

$$\mu^* = \mu_f (1 + 2.5\Theta_f + 10.05\Theta_f^2 + 0.00273e^{16.6\Theta_f}) \quad (2.3)$$

2.2. Particle-Phase Equations

The evolution of particle-phase is governed by a Liouville equation for the particle distribution function $\Phi(\mathbf{x}_p, \mathbf{u}_p, \rho_p, V_p, t)$

$$\frac{\partial \Phi}{\partial t} + \nabla_{\mathbf{x}} \cdot (\Phi \mathbf{u}_p) + \nabla_{\mathbf{u}_p} \cdot (\Phi \mathbf{A}_p) = 0, \quad (2.4)$$

where \mathbf{x}_p is the particle position, \mathbf{u}_p particle velocity, ρ_p particle density, and V_p particle volume. \mathbf{A}_p is the particle acceleration and $\mathbf{F}_p = m_p \mathbf{A}_p$ the total force acting on the particle of mass m_p and are given below. Here, $\nabla_{\mathbf{x}} \cdot$ and $\nabla_{\mathbf{u}_p} \cdot$ are the divergence operators with respect to space and velocity, respectively. The individual particle positions and velocities can be obtained by solving the Liouville equation in Lagrangian framework for each particle p :

$$\frac{d}{dt}(\mathbf{x}_p) = \mathbf{u}_p \quad (2.5)$$

$$m_p \frac{d}{dt}(\mathbf{u}_p) = \mathbf{F}_p \quad (2.6)$$

2.2.1. Particle Forces

The main issue is to model the force on a particle. This may consist of the standard hydrodynamic drag force, dynamic pressure gradient, gradient of viscous stress in the fluid phase, a generalized buoyancy force, and inter-particle collision. The total acceleration of the particle A_p is given as,

$$A_p = D_p(\mathbf{u}_f - \mathbf{u}_p) - \frac{1}{\rho_p} \nabla p_p + \left(1 - \frac{\rho_f}{\rho_p}\right) \mathbf{g} + \mathbf{B}_p + \mathbf{A}_{cp} \quad (2.7)$$

Here \mathbf{B}_p is the generalized buoyancy force and \mathbf{A}_{cp} is the acceleration due to inter-particle forces. If $\rho_p \gg \rho_g$ the pressure gradient, viscous, and buoyancy terms are usually negligible. In the present study, the generalized buoyancy force is also neglected for simplicity. It is shown later that, even without the presence of this buoyancy force, one can obtain lift of particles in a shear flow. The drag force is caused by the motion of a particle through the gas. The standard expression for D_p is used

$$D_p = \frac{3}{8} C_d \frac{\rho_f}{\rho_p} \frac{|\mathbf{u}_f - \mathbf{u}_p|}{R_p} \quad (2.8)$$

where C_d is the drag coefficient and is given by (Gidaspow 1994; Andrews & O'Rourke 1996)

$$C_d = \frac{24}{Re} (1 + a Re_p^b) \Theta_f^{-1.8}, \quad \text{for } Re_p < 1000 \quad (2.9)$$

$$= 0.44 \Theta_f^{-1.8}, \quad \text{for } Re_p \geq 1000 \quad (2.10)$$

where C_d is the drag coefficient for spherical particles, $R_p = (3V_p/4\pi)^{1/3}$ is the particle radius. The particle Reynolds number (Re_p) is given as

$$Re_p = \frac{2\rho_f \Theta_f |\mathbf{u}_f - \mathbf{u}_p| R_p}{\mu_f}. \quad (2.11)$$

There is an indirect collective effect in this drag term: when there is a dense collection of particles passing through the fluid interphase momentum exchange term in equation

(2.2) will cause \mathbf{u}_g to approach the particle velocity, \mathbf{u}_p thus decreasing the drag on a particle, a drafting effect.

The probability function Φ integrated over velocity and mass gives the probable number of particles per unit volume at \mathbf{x} and t in the interval $(\mathbf{u}_p, \mathbf{u}_p + d\mathbf{u}_p)$, $(\rho_p, \rho_p + d\rho_p)$, $(V_p, V_p + dV_p)$. The particle volume fraction (Θ_p) is defined from the particle distribution function as,

$$\Theta_p = \int \int \int \Phi V_p dV_p d\rho_p d\mathbf{u}_p. \quad (2.12)$$

From continuity, the gas-phase volume fraction is obtained as $\Theta_f = 1 - \Theta_p$. The interphase momentum transfer function per unit volume in equation (2.2) is given as

$$\mathbf{F} = \int \int \int \Phi V_p \rho_p \left[D_p (\mathbf{u}_f - \mathbf{u}_p) - \frac{1}{\rho_p} \nabla p_p \right] dV_p d\rho_p d\mathbf{u}_p. \quad (2.13)$$

2.2.2. Collision Force

The acceleration of particles due to inter-particle interactions (A_{cp}) is an important term in dense particulate and two-phase flows. For dilute and lightly loaded configurations, the particle volume fraction (Θ_p) is small ($< 10\%$), the inter-particle collisions are negligible and probability of particles overlapping each other is low. For dense particulate flows, however, the particle volume fraction should not exceed the close-packing limit (which is usually around 0.6 for three-dimensional case). In the Eulerian-Eulerian approach for two-phase flows, this is ensured by force due to the gradient of interparticle stress in the averaged momentum equation for the particle phase (Gidaspow 1986; Gidaspow 1994). Same model was used in Eulerian-Lagrangian approach by Andrews & O'Rourke (1996), Patankar & Joseph (2001b), Snider *et al.* (1998), and Snider (2001). Accordingly, the expression for acceleration of particles due to collision (\mathbf{A}_{cp}) is

$$\mathbf{A}_{cp} = -\frac{1}{\Theta_p \rho_p} \nabla \tau \quad (2.14)$$

where τ is the interparticle stress that provides a pressure type force that prevents packing of particles beyond the close-packing limit. Expression for τ is given as (from Snider *et al.* (1998))

$$\tau = \frac{P_s \Theta_p^\beta}{\Theta_{cp} - \Theta_p} \quad (2.15)$$

where P_s has units of pressure, Θ_{cp} is the particle volume fraction at close packing and β is a constant. The values for P_s and β are obtained from Snider *et al.* (1998). In this model, the inter-particle acceleration due to particle collision is assumed to be independent of its size and velocity. This model is least expensive in terms of computational cost as particle binary pairs are not formed and the collision force is directly obtained by interpolation from equation (2.14). This model, however, couldn't completely prevent the particle volume fraction to exceed the close packing limit and some numerical instabilities were experienced in the present unstructured code. Further research on this model will be conducted to eliminate this problem. An alternative but expensive collision scheme based on the distinct element method (DEM) of Cundall & Strack (1979). This scheme can be readily applied to parcel techniques used in Lagrangian spray simulations. A parcel represents a number (N_p) of droplets/particles of same size, velocity, and other properties. The effective radius (R_{par}) of a parcel based on its total volume is then given

by

$$R_{par} = \left(\frac{3N_p V_p}{4\pi} \right)^{1/3} \quad (2.16)$$

In this method, the interaction among particles and between wall and particles is taken into account separately to ensure that $\Theta_p \leq \Theta_{cp}$. The force F_{pj}^{P-P} on parcel p due to collision with parcel j is given by

$$\begin{aligned} F_{pj}^{P-P} &= 0 \quad \text{for } d_{pj} \geq (R_{par,p} + R_{par,j} + \alpha) \\ &= \left(k_c \delta_{pj}^{3/2} - \eta_c (\mathbf{u}_p - \mathbf{u}_j) \cdot \mathbf{n}_{pj} \right) \mathbf{n}_{pj} \quad \text{for } d_{pj} < (R_{par,p} + R_{par,j} + \alpha) \\ \delta_{pj} &= (R_{par,p} + R_{par,j} + \alpha) - d_{pj} \\ F_{jp}^{P-P} &= -F_{pj}^{P-P} \end{aligned}$$

where d_{pj} is the distance between the center of the p^{th} and j^{th} parcels, \mathbf{n}_{pj} is the unit vector from the center of parcel j to that of parcel p , α is the force range, k_c the stiffness parameter, and η_c the damping parameter. Tsuji *et al.* (1993) used the following expressions to compute the damping parameter

$$\begin{aligned} \eta_c &= 2\alpha \sqrt{\frac{m_p k_c}{1 + \alpha^2}} \\ \alpha &= -\ln(e/\pi) \end{aligned}$$

where e is the coefficient of restitution. Similarly, the parcel-wall force (F_{pw}^{P-W}) on parcel p due to collision with wall w is

$$\begin{aligned} F_{pw}^{P-W} &= 0 \quad \text{for } d_{pw} \geq (R_{par,p} + \alpha) \\ &= \left(k_c \delta_{pw}^{3/2} - \eta_c (\mathbf{u}_p) \cdot \mathbf{n}_{pw} \right) \mathbf{n}_{pw} \quad \text{for } d_{pw} < (R_{par,p} + \alpha) \\ \delta_{pw} &= (R_{par,p} + \alpha) - d_{pw} \end{aligned}$$

where d_{pw} is the distance between the parcel and the wall, and \mathbf{n}_{pw} is the unit vector from the wall to the center of the parcel. The total collision force is obtained by looping over all particles and walls. The corresponding particle acceleration is obtained by dividing the collision force by parcel mass ($m_p = N_p \rho_p V_p$).

3. Numerical Method

The collocated, finite-volume numerical scheme on unstructured grids developed by Mahesh *et al.* (2003) is modified to take into account the gas-phase volume fraction. In addition, the particle centroids are tracked using the Lagrangian framework developed by Apte *et al.* (2003b). The important feature of the numerical scheme is the computation of Θ_f and Θ_p on the unstructured grids. As the particles in the simulations performed do not move out of the domain or are destroyed, the total volume occupied by the particles remains constant from mass-conservation. As a particle crosses a particular control volume, its contribution to the particle volume fraction on neighboring cells must provide global mass-conservation. In addition, it was observed that the Eulerian volume fraction field should also be smooth in order to avoid numerical instabilities encountered due to changes in Θ as the particles move from one grid cell to another. A strategy similar

Computational domain, $0.2 \times 0.6 \times 0.0275m$	Grid, $10 \times 30 \times 5$
Fluid density, $1.254kg/m^3$	Particle Density, $2500kg/m^3$
Numer of Parcels, 2880	Particles per parcel, 3375
Diameter of particles, $500\mu m$	Initial particle concentration, 0.4

TABLE 1. Parameter description for the gravity-dominated sedimentation case.

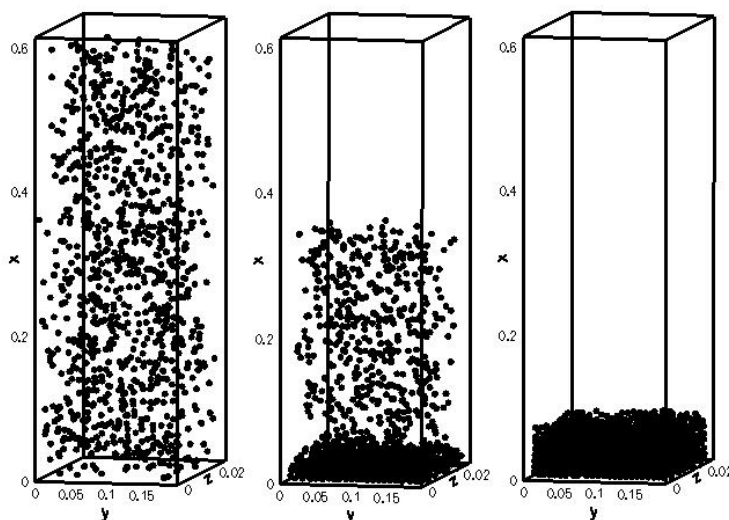


FIGURE 2. Temporal evolution particle distribution during gravity-dominated sedimentation. Initially the particles are randomly distributed over the box rectangular box.

to the two-way coupling methodology by Maxey & Patel (2001) is used to compute the volume fraction. The interphase momentum transport terms are also treated in a similar way.

The particle equations are integrated using third-order Runge-Kutta schemes for *ode*-solvers. At each Runge-Kutta step, the particles were located and the collision force was re-computed. This was found necessary to ensure that the close-packing limit for particle-volume fraction is not exceeded.

4. Results

We first simulated sedimentation of solid particles under gravity in a rectangular box. Details of this case are given in Table 1. The initial parcel positions are generated randomly in the top half of the box, $0.3 \leq y \leq 0.6$. These particles are then allowed to settle

Computational domain, $0.2 \times 0.6 \times 0.0275m$	Grid, $10 \times 30 \times 5$
Gas jet velocity, $9m/s$	Jet diameter, $0.04m$
Fluid density, $1.254kg/m^3$	Particle Density, $2500kg/m^3$
Numer of Parcels, 2880	Particles per parcel, 3375
Diameter of particles, $500\mu m$	Initial particle concentration, 0.4

TABLE 2. Parameter description for the simulation of fluidization by a gas jet.

through the gas-medium under gravity. The collision model is important here near the bottom wall after the initial group of parcels hit and bounce back from the bottom wall. This prevents particle volume fraction to exceed the close-pack limit. The upper mixture interface between the particles and the fluid is closely approximated by $h = gt^2/2$ similar to that obtained by Snider (2001). The particles eventually settle down with close-packing near the bottom wall. Snider (2001) and Patankar & Joseph (2001a) did sedimentation under gravity, in an inclined pipe with large number of parcels and used the particle stress model for collision force. This allowed them to use large number of parcels as the computational cost for this collision model is negligible. We plan to use this model to do similar validation test cases using the unstructured LES code. One difficulty at the time of writing was that this model didn't always prevent the particle volume fraction from exceeding the close-pack limit. Further investigations on this matter will be performed.

4.1. Gas-Solid Fluidization

We consider the problem of fluidization of solid particles arranged in an array at the bottom of a rectangular box. Fluidization is achieved by a jet of gas issuing from the bottom of the box. The flow parameters are given in Table 2. The choice of collision parameters is based on the recent computations by Patankar & Joseph (2001b). The particle motion is mostly dominated by the hydrodynamic drag force and collision model should not affect the overall particle motion. The collision model, however, is important in governing the particle behavior near the walls and helps prevent the volume fraction from exceeding the close-pack limit.

Figure 3 shows the position of parcels at different times during bubbling fluidization. Parcel diameters are drawn to scale. The jet issuing from the bottom wall pushes the particles away from the center region and creates a gas-bubble in the center. The particles collide with each other and the wall and are pushed back towards the central jet along the bottom wall. They are then entrained by the jet and are levitated. This eventually divides the central bubble and two bubbles are trapped. The particles tend to move upwards and collide with the upper wall and remain levitated during future times. The computational results are in good agreement with the simulations of Patankar & Joseph (2001b) as well as in qualitative agreement with experiments on jet fluidization. Similar results are reported using Eulerian-Eulerian approach in two-dimensions by Ding & Gidaspow (1990).

4.2. Fluidization by Lift of Spherical Particles

The transport of particles by fluids in coal-water slurries, hydraulically fractured rocks in oil-bearing reservoirs, bedload transport in rivers and canals and their overall effect on the river bed erosion etc., are important scientific and industrial issues in particulate flows. In order to understand fluidization/sedimentation in such conduits, (Choi & Joseph 2001) performed a DNS study of fluidization of circular cylinders (300 particles) arranged

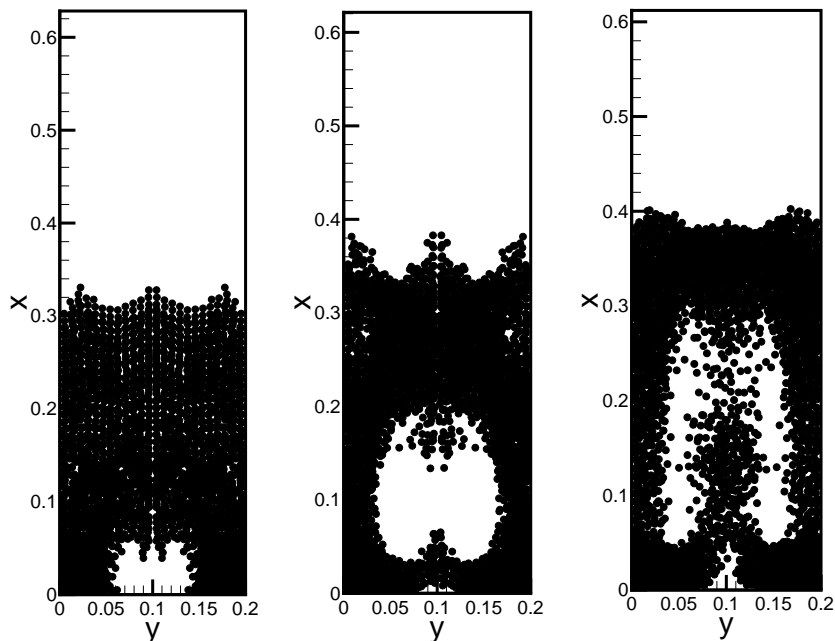


FIGURE 3. Temporal evolution of particle distribution during fluidization by a gas jet. Initially all the particles are uniformly arranged in layers at the bottom of the rectangular box. Air is injected through a rectangular slot at the bottom wall. Air bubbles are trapped within the particles and the growth and pattern of these bubbles are in agreement with experimental observations.

Computational domain, $63 \times 12 \times 12\text{cm}$	Grid, $20 \times 11 \times 10$
Gas jet velocity, 9m/s	Jet diameter, 0.04m
Fluid density, 1g/cm^3	Fluid viscosity, 1poise
Particle Density, 1.01g/cm^3	Diameter of particles, 0.95cm
Numer of Parcels, 3780	Particles per parcel, 1
Initial array height, 4.75cm ,	Initial centerline velocity, 360cm/s
Pressure gradient, 20dyne/cm^3	

TABLE 3. Parameter description for the simulation of fluidization of spherical particles in a plane Poiseuille flow.

at the bottom of a channel in plane Poiseuille flow. They observed that with sufficient pressure gradient across the channel, the particles initially at rest in the lower half of the channel start moving and roll over the wall. Particle rotation in a shear flow generates lift and the channel is fluidized after some time. We attempt to capture this phenomenon by our Eulerian-Lagrangian model. The flow parameters are given in Table 3. As opposed to Choi & Joseph (2001), we are performing three-dimensional simulations and our particles are spheres. As shown in Fig.4 we observe that the effect of volume displacement due

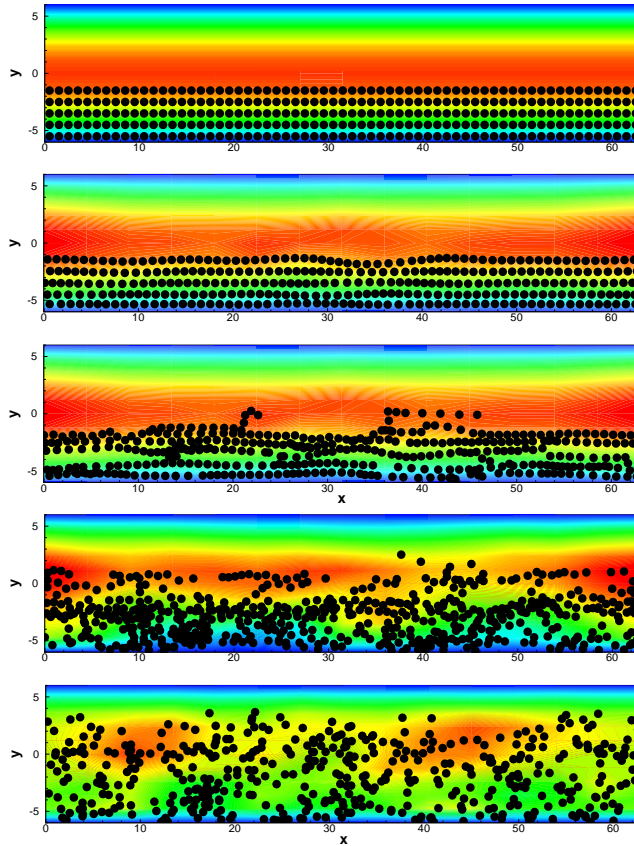


FIGURE 4. Temporal evolution of particle distribution during fluidization by lift in a plane Poiseuille flow. Also shown are contours of axial gas-phase velocity. Initially all particles are arranged at the bottom of the channel.

to particles is to set up Kelvin-Helmholtz type waves between the fluid and particle layers. A vertical pressure gradient is created and gives vertical velocity to the particles and the channel gets fluidized. We also did several test cases, with higher grid resolution, increased density ratios to obtain similar results. With increased particle density, the two-way coupling between the particle and fluid momentum equation, decelerates the fluid in the bottom half of a channel and an inflection point is created in the axial velocity profile. This eventually cause lift and particle dispersal. In liquid-fuel combustor applications, we believe that similar mechanism can be observed in the dense-spray regime near the injector and will allow us to capture the important features of primary atomization.

5. Summary

We have developed a numerical scheme which accounts for the displacement of the fluid by particles and is applicable to dense particulate flows and spray regimes close to the nozzle injector. This scheme has been implemented into the unstructured LES code. We performed various numerical simulations of fluidization and particulate flows to validate our scheme. It was shown through simulation of channel flow with layers of spherical

particles at the bottom wall that the effect of particle volume fraction is to displace the fluid in a control volume and create vertical pressure gradient through two-way coupling between the particles and fluid. This gives Kelvin-Helmholtz type instability waves which result in dispersal and lift-off of particles. This liftoff of dense-particles cannot be observed without explicit modeling of lift-forces on particles by using the standard point-particle approximation in Lagrangian-Eulerian framework. Similar K-H waves are present in the dense spray regime near the injector nozzle which may affect the overall spray dynamics and breakup in practical combustors. We plan to apply this model coupled with secondary breakup model to perform simulations of spray atomization. We also plan to perform several validation studies of this methodology for dense particulate/granular flows to address some issues related to collision scheme, efficient and consistent computation of particle volume fraction on multiple domain-decomposition.

6. Acknowledgement

Support for this work was provided by the United States Department of Energy under the Accelerated Strategic Computing Initiative (ASCI) program. We also thank Prof. Parviz Moin and Dr. Nagi Mansour for useful discussions as well as for providing support to perform this work.

REFERENCES

- ANDREWS, M. J., & O'ROURKE, P. 1996 The multiphase particle-in-cell (MP-PIC) method for dense particle flow. *Int. J. Mult. Flow* **22**, 379-402.
- APTE, S. V., GOROKHOVSKI, M. & MOIN, P. 2003a LES of atomizing spray with stochastic modeling of secondary breakup *Int. J. Mult. Flow* **29**, 1503-1522.
- APTE, S. V., MAHESH, K., MOIN, P., & OEFELEIN, J.C. 2003b Large-eddy simulation of swirling particle-laden flows in a coaxial-jet combustor. *Int. J. Mult. Flow* **29**, 1311-1331.
- CHOI, H.G., & JOESPH, D.D. 2001 Fluidization by lift of 300 circular particles in plane Poiseuille flow by direct numerical simulation. *J. Fluid. Mech.* **438**, 101-128.
- CUNDALL P.A., & STRACK, O.D.L. 1979 A discrete numerical model for granular assemblies. *Geotechnique* **29**, 47-65.
- DING, J. & GIDASPOW, D. 1990 A bubbling fluidization model using kinetic theory of granular flow. *AIChE* **36**, 523-537.
- DUKOWICZ, J. K. 1980 A particle-fluid numerical model for liquid sprays. *J. Comput. Phys.* **35**, 229-253.
- GIDASPOW, D. 1986 Hydrodynamics of fluidization and heat transfer supercomputer modeling *Appl. Mech. Rev.* **39**, 1.
- GIDASPOW, D. 1994 Multiphase flow and fluidization continuum and kinetic descriptions. Academic Press, Boston, MA.
- HERRMANN, M. 2003 Modeling primary breakup: A three-dimensional Eulerian level set/vortex sheet method for two-phase interface dynamics. *Annual Research Briefs*, Center for Turbulence Research.
- JOSEPH, D.D., & LUNDGREN, T. 1990 Ensemble averaged and mixture theory equations for incompressible fluid-particle suspensions. *Int. J. Mult. Flow* **16**, 35-42.
- MAHESH, K., CONSTANTINESCU, G., & MOIN, P. 2003 A new time-accurate finite-

- volume fractional-step algorithm for prediction of turbulent flows on unstructured hybrid meshes. *J. Comput. Phys.*, to appear.
- MAXEY, M.R., & PATEL, B.K. 2001. Localized force representations for particles sedimenting in Stokes flow. *Int. J. Mult. Flow* **27**, 1603-1626.
- PATANKAR, N. A., & JOSEPH, D. D. 2001a Modeling and numerical simulation of particulate flows by the Eulerian-Lagrangian approach. *Int. J. Multi. Flow* **27**, 1659-1684.
- PATANKAR, N. A., & JOSEPH, D. D. 2001b Lagrangian numerical simulation of particulate flows. *Int. J. Multi. Flow* **27**, 1685-1706.
- SNIDER, D. M. 2001 An incompressible three-dimensional multiphase particle-in-cell model for dense particulate flows. *J. Comput. Phys.* **170**, 523-549.
- SNIDER, D. M. 1998 Sediment flow in inclined vessels calculated using multiphase particle-in-cell model for dense particle flow. *Int. J. Mult. Flow* **24**, 1359.
- SUSSMAN, M., SMEREKA, P. & OSHER, S. 1994 A level set approach for computing solutions to incompressible two-phase flow. *J. Comput. Phys.* **114**, 146-159.
- THOMAS, D.G. 1965 Transport characteristics of suspension: VIII. A note on the viscosity of Newtonian suspensions of uniform spherical particles. *J. Colloid. Sco.* **20**, 267-277.
- TRYGGVASON, G., BUNNER, B. ESMAEELI, A., JURIC, D., AL-RAWAHI, N., TAUBER, W., HAN, J., NAS, S. & JAN, Y.-J. 2001 A Front-Tracking Method for the Computations of Multiphase Flow *J. Comput. Phys.* **169**, 708-759.
- TSUJI, Y., KAWAGUCHI, T., & TANAKA, T. 1993 Discrete particle simulation of 2-dimensional fluidized-bed. *Powder Technology* **77**, pp. 79-87.